www.itcon.org - Journal of Information Technology in Construction - ISSN 1874-4753

HAZARDS, VULNERABILITY AND INTERACTIONS AT CONSTRUCTION SITES: SPATIAL RISK MAPPING

SUBMITTED: April 2016.
REVISED: November 2016
PUBLISHED: January 2017 at http://www.itcon.org/2017/4
EDITOR: Turk Ž.

Mohammed Abunemeh, PhD student,
Institut de Recherche en Constructibilité, ESTP, Université Paris-Est, F-94230, Cachan, France;
mabu@estp-paris.eu

Rani El meouche, Associate Professor, (corresponding Author)
Institut de Recherche en Constructibilité, ESTP, Université Paris-Est, F-94230, Cachan, France;
relmeouche@estp-paris.eu

Ihab Hijaze, Assistant Professor,
Urban Planning Engineering Department, An-Najah National University, P.O. Box: 7, West Bank, Palestine;

Ahmed Mebarki, Professor,
Lab. Modélisation et Simulation Multi Echelle (MSME / UMR 8208 CNRS),
Université Paris-Est, 5 Bd Descartes, 77454, Marne-La-Vallée, France;

Isam Shahrour, Professor,
Laboratoire de Génie Civil et géo-Environnement, Université Lille1, 59 650 Villeneuve d'Ascq, France;

SUMMARY: *Construction sites contain several supporting facilities that are required to perform construction activities. These facilities may be exposed to several hazards. This may lead to adverse consequences for the whole construction process, which in turn lead to fatal accidents that have a major impact on worker and employee productivity, project completion time, project quality and project budget. This paper proposes a framework to visualize spatial variability of a construction site's risk, generated by natural or technological hazard, through using hazard and vulnerability interaction matrices, between potential sources and potential surrounding targets. The proposed framework depends on using analytical hierarchy process (AHP), the potential global impact of facilities obtained from the interaction matrices, and the capabilities of GIS to generate results in the mapping form. The methodology is implemented in a real case project. The results show the capability of framework to visualize construction site risks due to natural or technological hazard, and also identify the most at risk position within a construction site.*

KEYWORDS: *Risk management, Natural or technological hazard, Construction site, AHP, GIS, Risk map*

REFERENCE: *Mohammed Abunemeh, Rani El meouche, Ihab Hijaze, Ahmed Mebarki, Isam Shahrour (2017). Hazards, vulnerability and interactions at construction sites: spatial risk mapping. Journal of Information Technology in Construction (ITcon), Vol. 22, pg. 63-79, http://www.itcon.org/2017/4*

1. INTRODUCTION

The construction industry is distinguished from other industries by the large amount of risks occurring during the execution of construction projects (Zhang et al., 2013). This refers to the participation of different parties with different goals; these parties spend a lot of time at construction sites. Therefore it is very important to organize a site adequately in order to facilitate and accelerate parties moving within and around the site as well as to save time and increase productivity and safety. (Zolfagharian and Irizarry, 2014) stated that for each construction project, the site layout planning is distinctive from any other projects and depends entirely on the work areas and the location of different facilities.

Referring to (El-Rayes and Said, 2009) the construction site space is considered as one of the project resources that require management, like any other resources, in order to accomplish the project objectives. Though there are numerous researches dealing with site space management to smooth arrangement of conducting construction activities, some of construction site managers and planners still give less attention to site space management which still relies on the concept "first come first serve".

Site layout planning can be defined as the accommodation of temporary facilities that are required while performing construction activities, such as material storage, fabrication areas, and parking lots at a convenient location within the available site space. Therefore, it is important for the construction site manager to visualize the effect of the proposed site layout plan, with an efficient view of work spaces and the interaction among facilities, on the variability of risk within a construction site in order to enhance the decision making process especially in the case of an emergency, and assist in identifying the position at most risk within the site. Unfortunately, few efforts have been devoted to considering the impact of natural hazards and their risks on construction sites. The present study addresses three main topics:

- The loss of life as a result of construction accidents every year should be reduced. According to (Banaitiene and Banaitis, 2012), about 1300 people are being killed every year in Europe due to construction accidents. Furthermore, construction workers are about three times more likely to be killed and twice as likely to be injured compared to other industries.
- Construction companies that conduct risk management efficiently will benefit from greater productivity, financial savings, enhanced decision making and success rates of new projects.
- The hazards such as fire may take place at any facilities in construction site. It can then disseminate to other facilities or positions within the site, causing what is called domino-effect phenomena, which lead to catastrophic damages and losses in property and life. Even though this rarely happens in construction sites, the high dependence on advanced technology use which depends highly on electrical and fuel energy usage may increase the probability of natural hazards occurrence. It is then worth to consider natural hazard as one of other usual hazards happened during construction of project.

However, few studies tackled the risk of the fire hazard within a construction site. Thus, this research focuses and aims to enhance the visualization of global risk (generated from fire hazards) within a construction site by developing a new framework that takes into account the hazard and vulnerability interaction matrices between potential sources and potential surrounding targets. It is necessary to define the impact of one facility on another and the impact on the system as a whole in order to avoid fatal accidents that have a major impact on worker productivity, project completion time, project quality and project budget. Moreover, the visualization of risk due to fire hazards can be helpful in identifying the optimal routes to evacuate site seamlessly and without panic. Therefore guided crowd evacuation requires the identification of the highest risk areas (to avoid during evacuation when possible) and where is the lowest risk areas recommended for the evacuation.

2. LITERATURE REVIEW

Several studies have tackled the subject of construction risks and injuries occurring during the construction process, proposed methods to facilitate evacuation and reduce losses and casualties in cases of emergency, and the economic cost of implementing risk management while ignoring the impact of site layout on minimizing these losses.

(Kim et al., 2013) stated that the repetitive occurrence of similar accidents in construction disasters is a prevalent feature. They proposed an accident automated information retrieval system that extracts building information modeling objects and composes a query set by combining BIM objects with a project management information system. Users can markedly reduce query generation and can easily avoid risks by receiving similar past accident cases that may happen while they work. (Raz and Michael, 2001) developed a questionnaire to identify the tools that are most frequently utilized and contributed by enhancing project risk management.

(Akintoye and MacLeod, 1997) found that risk management during construction is very significant in reducing losses and increasing profitability, and also conclude that the risk analysis and management depends entirely on experience, judgement and intuition. They found that risk management techniques are rarely utilized due to a lack of knowledge and suspicion about the appropriateness of these techniques in giving the best results. (Carr and Tah, 2001) proposed a model for qualitative risk assessment based on a hierarchical risk breakdown structure. In this model, the relationship between project sources and consequences on project performance can be quantified utilizing a fuzzy approach.

(Charriere et al., 2012) talked about the importance of risk communication as one of procedures that should be conducted to enhance the preparedness of inhabitants in order to minimize risk disaster. They proposed a visualization utilizing GIS as one of the best ways of propagating information about spatial phenomena. (Belinfante et al., 2012) conducted a study to propose a way of determining the economic value of geospatial information in risk management. They claimed that the probable value of geo-information in risk management is high due to its ability to enhance the speed and quality of decision making in disaster and risk management, which in turn makes it possible to minimize losses and damage. (Kang et al., 2013) developed a risk management visualization model that has the capability to analyze the degree of risk in construction projects by collecting risk information utilizing quantifying methodologies like the Analytical Hierarchy Process (AHP) and fuzzy techniques.

(Elbeltagi and Hegazy, 2003) proposed a model for site layout planning considering both travel distance and site safety criteria; they presented the construction site and facilities as a multi-unit, and a genetic algorithm was used as the optimal means to get the optimal site layout. (Jannadi and Almishari, 2003) developed computerized model called risk assessor model (RAM), to identify the risk associated with specific construction activities. It is helpful for contractors in determining the highest risk of major construction activities and enhancing the safety precaution arrangements. (Mitropoulos and Namboodiri, 2010) proposed new safety risk assessment technique for construction activities called task demand assessment (TDA). It depends on the activity characteristics, level of observable task demand factors and exposure to the hazard. However, the method elucidated how the potential of accidents are highly impacted by the changes in the operation parameters of construction activities. Also it reveals the complexity to conduct activity safely. Although the previous two models are efficient, they focused only on hazard generated by construction activities. They did not consider the consequences of natural hazards that may lead to catastrophic destruction.

(Rozenfeld et al., 2010) developed a construction job safety analysis (CJSA) framework to assess the hazard of construction activities. The framework aims enhancing safety precautions and planning at the affected locations, through identifying the probable loss of control events for common construction activities, and their probability of occurrence. They found that the events related to exterior work at height are the most common. (Sousa et al., 2015) indicated that the rate of construction accidents is still very high, even with the resort to utilize advanced technology in performing construction activities. They referred this to the financial raise of applying additional safety precautions in a competitive market. Therefore, they offered a model that displays the cost- beneficial of conducting occupational safety and health risk management on construction projects.

(Mebarki et al., 2012a, 2014a; Mebarki and Barroca, 2014) performed a study considering the accidents that may be expected to happen in industrial plants. They stated that the domino effect will arise, and produce a catastrophic condition. (Gao et al., 2007) indicated that evacuation is very crucial in emergency management, and developed a model to minimize the evacuation time through performing a simulation of a route/time swapping process utilizing a heuristic algorithm to get the optimal solution.

It is obvious from this literature that little attention has been devoted to considering the impact of natural hazards (fire for instance) on the construction site configuration and the vulnerability of facilities in order to understand and visualize the spatial variability of risk at the construction site and to be able to avoid or at least reduce the domino effect of disaster. Therefore, the present research will focus on:

- The implementation of an interaction matrix technique, which has been attempted in environmental impact assessments and structural risk for informal masonry construction (Mebarki et al., 2012b), to determine the potential global impact for each construction facility on the project as a whole.
- The use of GIS capabilities to analyze spatial datasets and generate a risk map for a construction site, which will assist in identifying the most at risk positions within the site, which facilitate finding the best routes with minimum risk that should be followed to minimize injuries and victims.

3. RESEARCH METHODOLOGY

The proposed integrated framework is shown in FIG. 1: Methodology flowchart. It is obvious that two interaction matrices should be created for every expected natural or technological hazard at a construction site (earthquake, flood, tsunami, fire, explosion, leakage of hazardous materials, for instance, in the current research fire hazard is considered): one for the hazard generated from each source and another one for the vulnerability of the targets to the hazards presented by the sources. For the sake of simplicity, it is assumed, in this research, that the conditional vulnerability is a linear function of the hazard value; therefore the concentration is directed toward creating a hazard interaction matrix. The adaptation for other systems and hazards will therefore require the appropriate conditional vulnerability specific to the considered system.

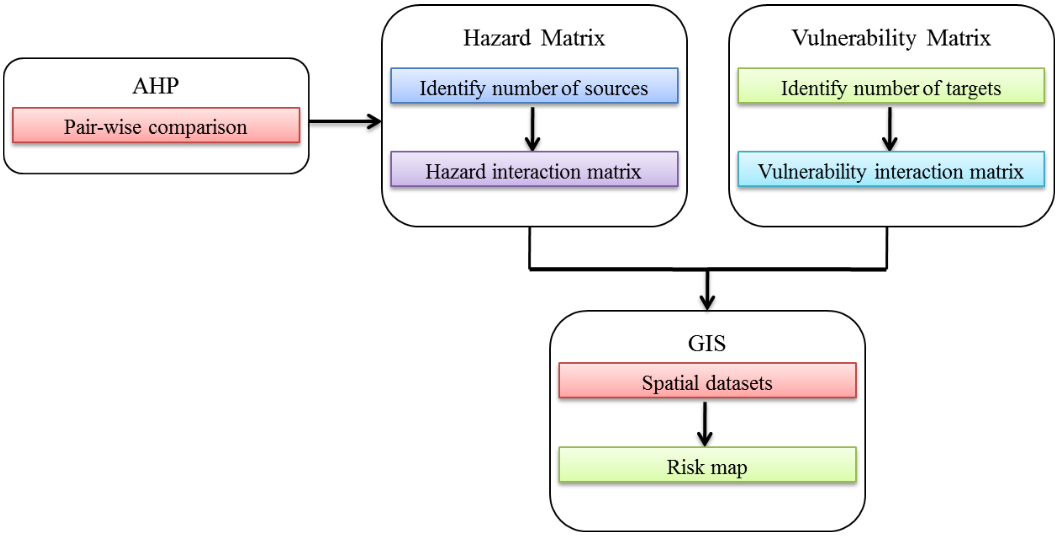

FIG. 1: Methodology flowchart

A pair-wise comparison utilizing an Analytical Hierarchy Process (AHP) will be conducted to evaluate the hazards generated from each source and the vulnerability of each target. Referring to (Saaty, 1980), AHP can afford relative priorities on a ratio scale for all objects based on both the decision maker's judgments and the consistency of these judgments. After that, regarding the hazard interaction scale measurement, the object that has the highest priority will take the largest hazard scale value, while the remaining objects will take values in proportion to the highest one, depending on their relative priorities. The hierarchy of model consist of two levels as shown in FIG. 2. Level one represents the main goal of the problem under consideration, whereas, level two represents the facilities that will be located in the sites. It is assumed that each facility represents a source of fire hazard. The experts are requested to conduct pairwise comparison among facilities (determining the fire hazard intensity for each facility). The fire intensity generated from each facility is not the same. It depends on the nature of facility, its usage and the presence and amount of combustible materials.

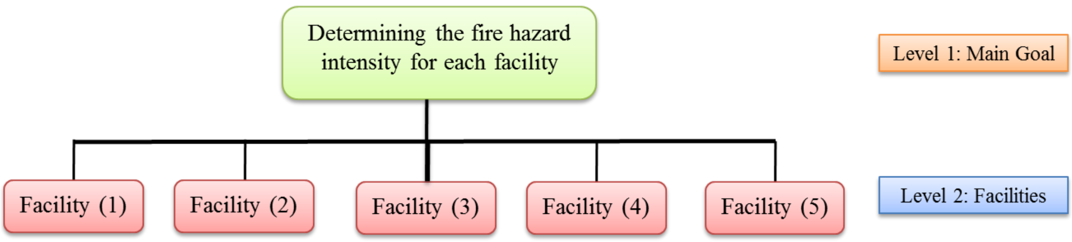

FIG. 2: The hierarchy levels of the model

The hazard sources (fire) are attributed to all present facilities in a construction site. This assumption considers the worst condition, where the fire occurred in all facilities at the same time. Actually, the fire hazard intensity generated from each facility is differ from one to another, therefore pairwise comparison is required to determine the relative hazard intensity of each facility with respect to other facilities at a higher level of the hierarchy. It is, thereafter, possible to hierarchy the facilities from the highest to the lowest based on the relative fire hazard intensity.

Finally the GIS will be helpful to generate results in map form. The proposed model aims at visualizing the spatial variability of risk generated by the natural or technological hazards within a construction site. Therefore, it is first required to identify the kind of hazard that will be taken into consideration. Once the hazard is identified, the next step is to perform pair-wise comparison and determine the relative hazard priorities for each object with respect to others in order to evaluate objectively the intensity of hazard generated by each potential source object within a construction site. Afterwards, the hazard interaction matrix will be developed and filled based on the results of the pair-wise comparisons and the hazards' attenuation value, which is determined based on the nature of the hazard (Mebarki et al., 2012a, 2012b). Thereafter, the risk is determined as a product between hazard and vulnerability; thus the risk interaction matrix will be created, from which the global potential risk for every object will be determined and will later be imported to the Geographic Information System (GIS) to generate and visualize the variability of risk within the construction site (see FIG. 1: Methodology flowchart).

3.1 Analytical hierarchy process (AHP)

AHP is a widespread decision making method. It is selected for use in this study due to its simplicity, flexibility, and its ability to determine the relative impact of numerous components on the predicted outcomes, as well as its ability to judge the rate of consistency of the judgment, while the most important thing is its capability to convert the subjective judgment into an objective one. The implementation of pair-wise comparison utilizing AHP involves: (1) determining the components that will exist at a construction site, (2) creating a pair-wise comparison matrix (size n x n) in which a construction manager or planner conducts the hazard judgment evaluation. According to (Saaty, 1994), pair-wise comparison is favoured because the decision maker performs the comparison between two components at the same time and it is done in terms of which component dominates the others. AHP pair-wise comparison uses the relative scale measurement shown in TABLE 1. Basically, the number of judgments required is equal to $\frac{n\,(n-1)}{2}$ and the reciprocals are automatically assigned for each pair-wise comparison. Afterwards, the relative priority of hazard intensity for each object with respect to others at the construction site is determined. Finally, the consistency of the judgment is examined by calculating a consistency ratio (CR) as specified by (Saaty, 1980), who indicated that if CR is greater than 0.1, then the judgments are not acceptable. Therefore, the results of the AHP will be meaningless and the judgment should be revised.

TABLE 1: The relative scale for AHP pair-wise comparison

Points scale	Description
1	Equal
3	Moderate
5	High
7	Very high
9	Extreme
2,4,6,8	Intermediate values; for example, a value of 6 means that the degree level is between high (5) and very high (7).

3.2 Interaction matrix

Herein, an explanation of the hazard interaction matrix will be presented. Interaction matrices were used in environmental impact assessment, where the features of the environment were recorded vertically, and the actions were listed horizontally (Mavroulidou et al., 2004). The interaction matrices can be utilized in order to identify the impact of one component on another within the system, the effect of the system on each component, and to determine the total impact for each component within the whole system, considering both the impact of the component on the system and the effect of the system on the component. Therefore, this kind of matrix is used in this study to identify the impact of each construction facility (crane, site offices, batch plant, etc.) within a construction site on another, and the potential global impact of that facility on the construction site as a whole, to be combined with a spatial dataset using GIS to generate a risk map. However, the size of the matrix varies from one construction site to another, depending on the number of construction facilities existing within the site (Mebarki et al., 2012a, 2012b, 2014a; Mebarki and Barroca, 2014).

3.2.1 Generating the interaction matrix (Hazard modelling)

Several steps should be followed in order to create a hazard interaction matrix (Mebarki et al., 2012a, 2012b, 2014a; Mebarki and Barroca, 2014):

- Identify the construction facilities that will be erected within the construction site.

- Identify the nature of hazard that may arise on a construction site (leakage of hazardous material, fire, earthquake effects, flood effects, explosions and blast waves, malicious acts etc.), in the current research the fire hazard is considered.
- Evaluate the hazard category generated by each facility compared to other facilities using the relative scale measurement categories specified in TABLE 2, where 0 represents the lowest hazard, while 4 represents the highest hazard, in order to create and fill the diagonal of the hazard interaction matrix. The results of pair-wise comparison have been used, where the facility with the highest priority will take the largest hazard scale value "4", while all the remaining facilities will take values in proportion to the highest one and depending on their relative priorities.
- Create a hazard interaction matrix that displays the source of hazard (i) and the its impact on target (j). In addition, fill the diagonal of the matrix with the evaluated hazard values, which represent the highest hazard from each source (i), as shown in FIG. 3, where H_{11} represents the hazard generated from source 1, H_{ii} represents the hazard generated from source (i) and so on. These values are obtained from step 3. In fact, while this value seems such as the object interacting with itself, this just indicates that the intensity and consequence of the hazard is the highest at the object itself and attenuate as it becomes far away from the object.

$$\begin{array}{cc} & \text{Target (j)} \\ \text{Source}\,(i) & \begin{bmatrix} H_{11} & \cdots & \square \\ \vdots & H_{ij} & \vdots \\ \square & \cdots & H_{nn} \end{bmatrix} \end{array}$$

FIG. 3: The diagonal of the hazard interaction matrix

TABLE 2: Hazard interaction scale measurements

Hazard level	Details
0	No hazard
1	Low hazard
2	Moderate hazard
3	High hazard
4	Very high hazard

- For the sake of simplicity, it is assumed that there is a linear attenuation with distance, i.e. a linear relationship between the hazard interaction values H_{ij} and the distance d_{ij} to the target.

  Therefore, the hazard from source (i) on target (j) decreases as the target (j) becomes far away from source (i). Thus, the hazard decay, which is represented by the slope of linearity decreasing (tan α), should be identified as shown in FIG. 4 based on the nature of the hazard whether is it thermal flux, heat pressure or any other kind of hazard, and can be expressed using equations (1–7). In fact, specific studies of the attenuation can be adopted depending on the nature of the hazard (flood, explosion, or fire, for instance) (Mebarki et al., 2012a, 2012b, 2014a; Mebarki and Barroca, 2014). The current research will focus on the fire hazard.

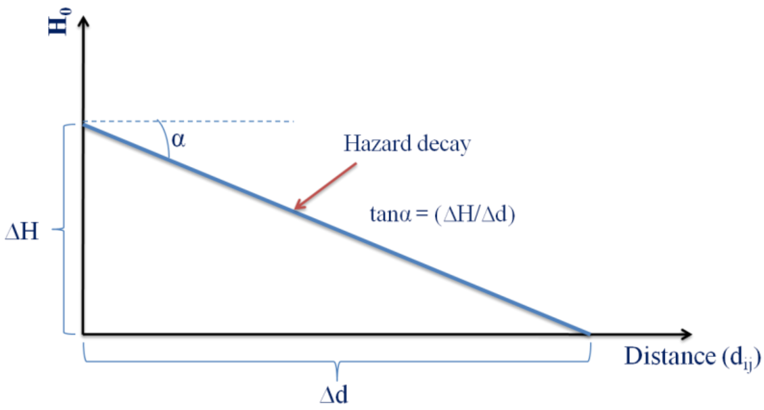

FIG. 4: Hazard decay with distance

$$f(h_{ij}) = h_{ij}|_{d=d_{ij}} = h_{ij}|_{d=0} + (\tan\alpha) * d_{ij} * \beta_{ij} \tag{1}$$

$$d_{ij} = \sqrt{(x_i - x_j)^2 + (y_i - y_j)^2} \tag{2}$$

$$\beta_{ij} = \begin{cases} 1, & \text{if } i \neq j \\ 0, & \text{otherwise} \end{cases} \tag{3}$$

$$\mathbf{H} = \begin{bmatrix} h_{11} & \dots & h_{1n} \\ \vdots & h_{ij} & \vdots \\ h_{n1} & \dots & h_{nn} \end{bmatrix} \tag{4}$$

$$\mathbf{H}^* = \begin{bmatrix} h^*_{11} & \dots & h^*_{1n} \\ \vdots & h^*_{ij} & \vdots \\ h^*_{n1} & \dots & h^*_{nn} \end{bmatrix} \tag{5}$$

$$h^*_{ij} = \frac{h_{ij}}{\max[h^0_i]} \tag{6}$$

$$\mathbf{H} = \max\left[h_{ij}|_{d=0}\right].\ \boldsymbol{H}^* = \max\left[h_{ij}|_{d=0}\right].\begin{bmatrix} h^*_{11} & \cdots & h^*_{1n} \\ \vdots & h^*_{ij} & \vdots \\ h^*_{n1} & \cdots & h^*_{nn} \end{bmatrix} \tag{7}$$

where: $h_{ij}|_{d=d_{ij}}$: is the hazard interaction value between facilities (i) and (j) at any distance (d) i.e. the effect of source (i) on target (j); **H**: is the hazard interaction matrix; $h_{ij}|_{d=0}$: is the maximum potential hazard generated from facility (i) at a distance d = 0, i.e. the hazard intensity at the object itself; $\frac{\Delta H}{\Delta d}$: is the amount of hazard attenuation with distance (hazard decay) depending on the nature of the hazard; β_{ij} : is a factor to consider that the hazard evaluation value is maximum at d = 0 (i.e. to consider the case when i = j); d_{ij} : is the Euclidean distance between facility (i) and (j); x_i, y_i, x_j, y_j: is the coordinates of facilities (i) and (j); n: is the total number of facilities in the construction site; $\boldsymbol{H}^*$: is the normalized hazard interaction matrix; h^*_{ij} : is the normalized hazard interaction value between facilities (i) and (j), $\forall\, h^*_{ij} \in [0,1]$; $max\left[h_{ij}|_{d=0}\right]$: is the maximum value of potential hazard generated from facility (i) at distance 0 among all facilities, i.e. the maximum value among all diagonal values in the hazard interaction matrix.

3.2.2 Generating the interaction matrix (Vulnerability modelling)

Once the hazard interaction matrix is created, it is crucial to identify the vulnerability of all of the targets within a site to the hazards generated from each source. The vulnerability of each target depends on its capacity to resist various hazard values generated by surrounding sources. Vulnerability represents the potential weakness of whole targets to the hazard generated from each source. Also, physical vulnerability is the degree of loss to a given element at risk resulting from the occurrence of a natural phenomenon (fire in our case) of a given intensity and expressed on scale from 0 (no damage) to 1 (completely damage). In the present research, the vulnerability is expressed as function of hazard intensity. It is assumed that the conditional vulnerability is a linear function of the hazard value due to lack of vulnerability curves for supporting facilities (elements at risk), as shown in FIG. 5. A linear variation of the conditional vulnerability is adopted for the sake of simplicity and can be expressed as shown in equations (8-12). However, equation (9) indicates that the target limit state occurs when the hazard generated from source (i) and the impact on the potential target (j) are equal to the vulnerability of potential target (j) subject to the hazard generated from source (i). For real cases, each target should have its specific fragility curve and vulnerability, according to its constitutive materials and to its physical response to the various hazards generated within the layout. A physical analysis is able therefore to provide the response of the target and its capacity to withstand the various hazard levels.

$$\mathrm{V_{ji}} = f(\mathrm{H_{ij}})\text{: conditional values of the vulnerability} \tag{8}$$

Therefore,

$$\begin{cases} \mathrm{V_{ji}} < \mathrm{H_{ij}}\text{: Conditional failure of the target} \\ \mathrm{V_{ji}} > \mathrm{H_{ij}}\text{: Conditional safety of the target} \\ \mathrm{V_{ji}} = \mathrm{H_{ij}}\text{: Target limit state safety} \end{cases} \tag{9}$$

$$\mathrm{V} = \begin{bmatrix} \mathrm{v_{11}} & \cdots & \mathrm{v_{1n}} \\ \vdots & \mathrm{v_{ji}} & \vdots \\ \mathrm{v_{n1}} & \cdots & \mathrm{v_{nn}} \end{bmatrix} \tag{10}$$

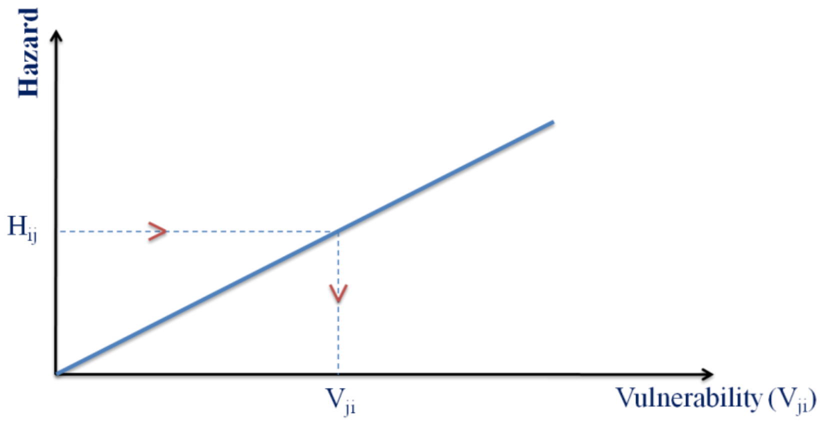

FIG. 5: Vulnerability as a function of hazard value.

Since the vulnerability is assumed as function of hazard as shown in FIG. 5, then:

$$\mathrm{v}_{ji}^{*} = \mathrm{h}_{ij}^{*} \tag{11}$$

$$\mathrm{V} = \mathrm{H^T} \tag{12}$$

Where $\mathrm{H_{ij}}$: is the hazard evaluation value generated from source (i) and the impact on target (j); $\mathrm{v_{ji}^*}$: is the normalized vulnerability of target (j) to the hazard generated by source (i); V: is the vulnerability interaction matrix; $\mathrm{H^T}$: is the hazard transpose interaction matrix

3.2.3 Generating the interaction matrix (Risk modelling)

The supporting facilities that will be erected in the construction site represent the elements at risk. The potential risk (r_{ij}), resulted from the hazard of source (i) on target (j) and the vulnerability of target (j) to that hazard, quantifies the probability of failure or damage for that target. It is estimated as a convolution product of both the hazards generated by the sources and the targets' vulnerability. Therefore, the risk interaction matrix can be developed. Also, the potential risk resulted from the hazard and vulnerability interactions among facilities can be identified utilizing equation (13):

$$Potential\ risk\ (r_{ij}) = \mathrm{h_{ij}} .\ \mathrm{v_{ji}} \tag{13}$$

Once the risk interaction matrix is created, the impact of all other facilities on a specific facility and the impact of each facility on the system as a whole are identified, as explained in the following section 3.3, by implementing the matrix algebra through:(1)Find the summation of each individual row and the summation for each individual column in the matrix (the row summation expresses the potential risk of source (i) at the construction site, while the column summation expresses the potential sensitivity of each target (j) to the total risks and threats); (2) Then, combine the above two summations to determine the global potential risk of each source (i) on the whole plant (i.e. determine the overall weight or interaction of each facility within the construction site); (3) Furthermore, the risk should be normalized with values ranging within [0–1] so that it has a probabilistic meaning. It therefore becomes a probability of failure or accident. A probabilistic combination of facilities' failure is therefore easy to perform and the meaning of the risk becomes relevant as it can be associated with the expected loss or damage of the whole site.

3.3 Mathematical modelling of the risk interaction matrix

This section explains the derivation of the mathematical formulas adopted for this study. Consider a risk interaction matrix between construction facilities $\boldsymbol{\mathcal{R}} \in \mathcal{R}_n$ where (n) is the total number of construction facilities that will be accommodated within the construction site. Hence the (n x n) matrix will be developed as shown in equations (14–19):

$$\boldsymbol{\mathcal{R}} = \mathcal{R}_{\mathrm{max}}|_{\mathrm{V}} * \mathcal{R}^{*}{}_{\mathrm{ij}} = \mathcal{R}_{\mathrm{max}}|_{\mathrm{V}} . \begin{bmatrix} r^{*}_{11} & \cdots & r^{*}_{1\mathrm{n}} \\ \vdots & r^{*}_{\mathrm{ij}} & \vdots \\ r^{*}_{\mathrm{n}1} & \cdots & r^{*}_{\mathrm{nn}} \end{bmatrix} \tag{14}$$

Where: $\mathcal{R}_{\mathrm{max}}|_{\mathrm{V}}$ is the maximum potential risk evaluated within the system; $\mathcal{R}^{*}{}_{\mathrm{ij}}$ is the corresponding normalized risk, $\forall \mathcal{R}^{*}{}_{\mathrm{ij}} \in [0,1]$; r^{*}_{ij}: is the normalized potential risk, it is determined using equation 13. Once the risk interaction matrix has been created, the global potential risk of each facility within the system can be determined as follows:

$$\phi^{*}{}_{\mathrm{i},-} = \sum_{\mathrm{j}=1}^{\mathrm{n}} \mathrm{r_{ij}} \tag{15}$$

$$\phi^{*}{}_{-,\mathrm{j}} = \sum_{\mathrm{i}=1}^{\mathrm{n}} \mathrm{r_{ij}} \tag{16}$$

$$\varkappa^{*}{}_{\mathrm{i}} = \phi^{*}{}_{\mathrm{i},-} + \phi^{*}{}_{-,\mathrm{i}} \tag{17}$$

$$\psi_{\mathrm{i}} = \frac{\varkappa^{*}{}_{\mathrm{i}}}{\sum_{\mathrm{k}=1}^{\mathrm{n}} \varkappa^{*}_{\mathrm{k}}}, \tag{18}$$

$$\sum_{\mathrm{i}=1}^{\mathrm{n}} \psi_{\mathrm{i}} = 1, \quad \forall\, \mathrm{i} \in [\![1, \mathrm{n}]\!] \tag{19}$$

where: $\phi^{*}{}_{\mathrm{i},-}$: is the potential risk generated from each source (i) in the whole site (i.e. the potential risk of source (i) at the construction site); $\phi^{*}{}_{-,\mathrm{j}}$: is the potential sensitivity of each target (j) to the total risk from sources (the potential risk of all other facilities on the target j); $\varkappa^{*}{}_{\mathrm{i}}$: is the global potential risk of each source (i) on the whole site; ψ_{i} : is the relative global potential risk of each source (i) on the whole site (i.e. probability of failure of facility i). In the case where i = j, the value of r_{ij} will reflect the maximum risk generated from that source. All diagonal values in the matrix will have a maximum value compared to other values in the same row in the matrix, because the hazard generated from the source will have the highest influence on itself (at distance zero). Due to attenuation, this influence generally decreases as the target becomes far away from the hazard source, unless there is a local site effect and amplification.

3.4 GIS datasets

The relative potential global impact for each facility obtained from the risk interaction matrix is imported to GIS in order to perform a spatial analysis and generate a visual map of the risk within the construction site.

Therefore, the construction site and facilities will be converted to raster, and the potential global risk for each unknown node within the construction site can be estimated utilizing interpolation techniques based on the principle that spatially distributed elements are spatially correlated. One of these techniques that is common and widely used is inverse distance weighting (IDW), which is also adopted in this research. In order to guarantee that we determine the best estimated cell values and reliable results, the maximum number of points is used and their distribution within the site space has been considered. The average of the interpolated sample points is computed to estimate the unknown cell values as shown in equation (20). The IDW interpolation technique assumes that each interpolation point has an influence that reduces with distance, where the closer the estimated proximity of the sampled point to the unknown cell, the greater the influence it has in determining the average, as shown in equation (21). It appears from this equation that the diminution of the weight (the influence of the sampled point) will be greater at remote points than at nearby ones as the power value increases. Therefore, when the node becomes too close to the facilities with the highest potential global impact, the potential global risk at that node will be high compared to those located far away from these facilities.

$$\mathcal{Z}_k = \frac{\sum_{i=1}^{m} z_i w_{di}}{\sum_{i=1}^{m} w_{di}} \tag{20}$$

$$w_{di} = \frac{1}{d^p} \tag{21}$$

where: $\mathcal{Z}_k$: is the estimated potential global risk for each unknown node (k); z_i : is the value of the sample interpolated point (i); w_{di} : is the weight or influence of point (i) during the averaging process; d_i : is the distance between the sample interpolated point (i) and the unknown node (k) that is to be estimated; p: is the power value to be adopted; m: is the number of sample interpolated points used to estimate unknown node (k). FIG. 6 illustrates both equations (20 and 21) utilized for the interpolation process.

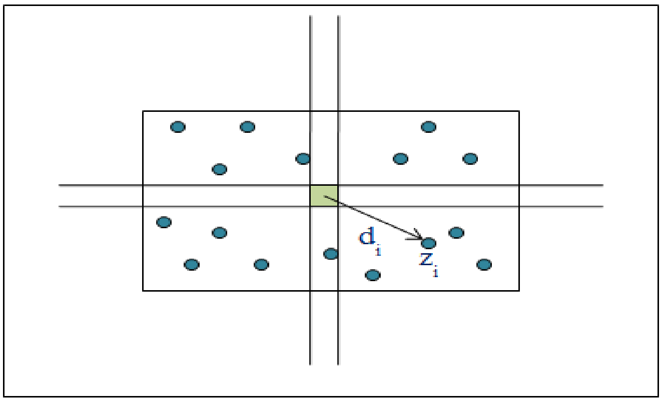

FIG. 6: Inverse distance weighted (IDW) interpolation process

4. MODEL IMPLEMENTATION

A real case study is implemented in order to clarify the ability of the proposed framework to visualize risk at a construction site, the metric system was used. The project consists of constructing two buildings with a total ground area equal to 2500 m^2. The nature, location and dimensions of the facilities are presented in TABLE 3 and the construction site boundaries and the existing facilities layout are shown in FIG. 7.

The proposed model requires the construction and safety managers to determine several inputs: (1) identify the kind of hazard, in the current project the fire hazard is considered; (2) identify the hazard attenuation value (hazard decay); (3) and finally identify the potential hazard and threat (hazard intensity) generated by each facility, by conducting pair-wise comparisons among them in order to find the overall priorities of facilities in term of fire hazard.

In this project the hazard is identified to be fire hazard with a hazard attenuation value equal to 0.01. Basically, the facilities in this project were divided into two categories: permanent facilities like buildings (F_{16} and F_{17}) and temporary facilities like (F_1 to F_{15}). The managers conduct pair-wise comparisons only among the temporary facilities, of which there are 13, i.e. they considered using either of the Y entity offices (F_5 or F_6) as representative of both because they have the same characteristics, and the same applies for the X entity temporary offices (F_7 or F_8). The managers were not considered permanent facilities in the pair-wise comparison, since permanent facilities do not exist from the commencement of the project, but it is proposed to assign them a moderate hazard value after they become present. Therefore, the hazards generated from buildings were assigned a value equal to 2. The other temporary facilities of the project were assigned hazard values depending on the pair-wise comparison analysis and results, where the facility with the highest priority will take the largest hazard scale value "4", while all the remaining facilities will take values in proportion to the highest one and depending on their relative priorities. Whatever the case, it is possible to insert permanent facilities in a pair-wise comparison process. Basically, according to (Saaty, 1980), the total number of comparisons required among the facilities is equal to $\frac{n\,(n-1)}{2}$. Thus in this project 78 comparisons were conducted ($\frac{13\,(13-1)}{2}$ = 76).

TABLE 3:Facilities descriptions, dimensions and locations

Facility	Description	Length (m)	Width (m)	Location coordinate (m) *
F_1	Electric generator	2	1	(62.59,103.74)
F_2	Tower crane	8	8	(62.30,109.14)
F_3	Y entity storage	6	3	(92.59,78.39)
F_4	Y entity storage & office	12	2.5	(88.84,73.79)
F_5	Y entity office 1	6	2.5	(94.70,65.50)
F_6	Y entity office 2	6	2.5	(100.34,66.35)
F_7	X entity temp office 1	12	3	(101.22,76.08)
F_8	X entity temp office 2	12	3	(100.53,71.89)
F_9	X entity offices	32	23	(110.08,101.14)
F_{10}	Container office	10	3.2	(59.21,26.89)
F_{11}	Concrete plant	14	6.5	(78.54,116.51)
F_{12}	Steel rebar storage	24	8	(74.01,89.47)
F_{13}	Steel workshop fabrication	20	9	(80.08,60.94)
F_{14}	Labor services	7	2.5	(30.67,76.92)
F_{15}	Parking lot	22	8	(92.92,126.22)
F_{16}	Building 1	50	26	(42.36,136.36)
F_{17}	Building 2	50	24	(53.76,78.72)

* The coordinates represent the center point of the facility

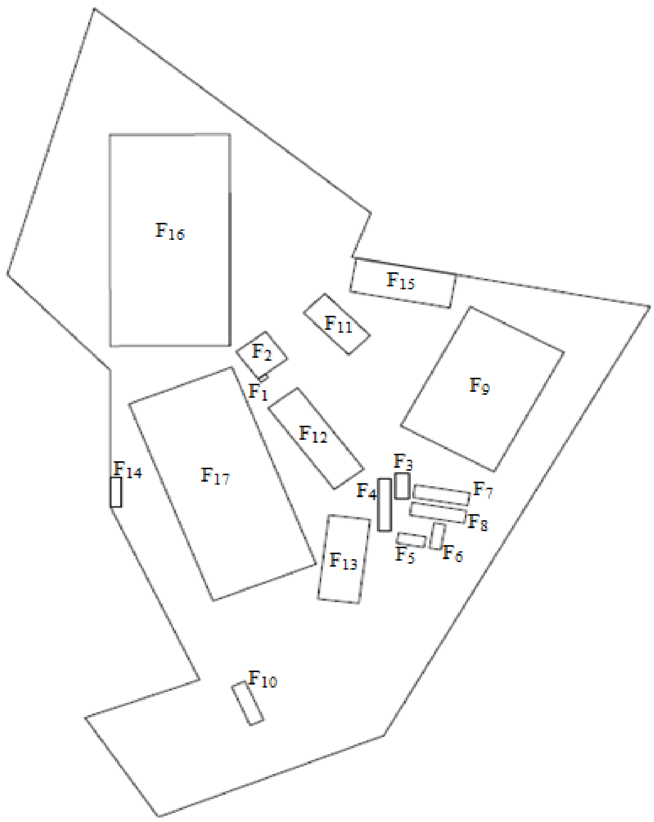

FIG. 7: Construction site layout

The Expert Choice software was utilized to identify the hazards and the relative priority of each facility with respect to others at a higher level of hierarchy. FIG. 8 and FIG. 9 display the 13x13 pair-wise comparison matrix among facilities to estimate relative fire intensity for each one, and the relative priorities of the facilities according to main goal of hierarchy, respectively. It is obvious from FIG. 9 that the electric generator has the highest priority value, which means that this facility will have the highest fire hazard intensity compared to others. Thus, it is assigned a hazard intensity value equal to 4 and all the others will be in proportion to it, based on their priorities as shown in TABLE 6. This latter presents the hazard intensity for each facility. The managers are required to review their comparisons and conduct the necessary adjustments if there is an inconsistency greater than 0.1. FIG. 9 also presents the inconsistency value equal to 0.03, which is less than 0.1; therefore the results are satisfactory and acceptable.

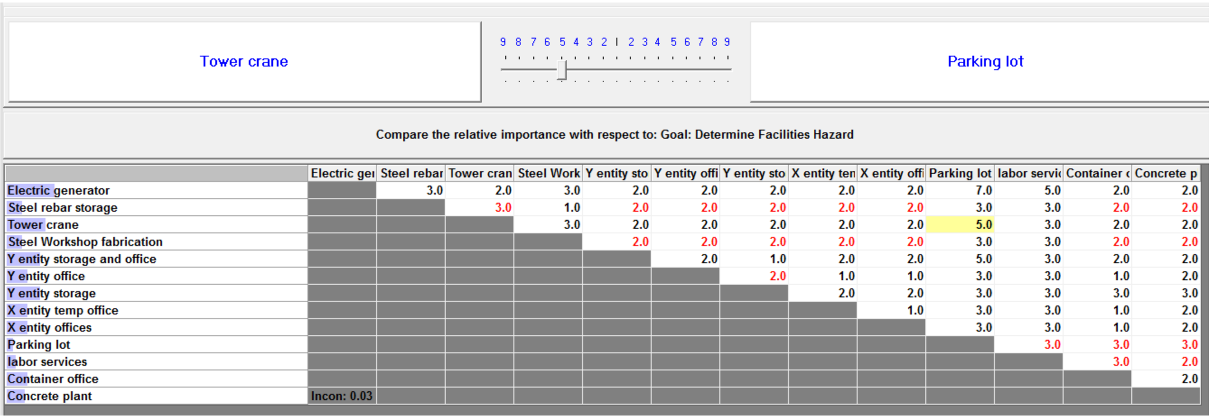

	Electric gei	Steel rebar	Tower cran	Steel Work	Y entity sto	Y entity offi	Y entity sto	X entity ten	X entity offi	Parking lot	labor servi	Container c	Concrete p
Electric generator		3.0	2.0	3.0	2.0	2.0	2.0	2.0	2.0	7.0	5.0	2.0	2.0
Steel rebar storage			3.0	1.0	2.0	2.0	2.0	2.0	2.0	3.0	3.0	2.0	2.0
Tower crane				3.0	2.0	2.0	2.0	2.0	2.0	5.0	3.0	2.0	2.0
Steel Workshop fabrication					2.0	2.0	2.0	2.0	2.0	3.0	3.0	2.0	2.0
Y entity storage and office						2.0	1.0	2.0	2.0	5.0	3.0	2.0	2.0
Y entity office							2.0	1.0	1.0	3.0	3.0	1.0	2.0
Y entity storage								2.0	2.0	3.0	3.0	3.0	3.0
X entity temp office									1.0	3.0	3.0	1.0	2.0
X entity offices										3.0	3.0	1.0	2.0
Parking lot											3.0	3.0	3.0
labor services												3.0	2.0
Container office													2.0
Concrete plant	Incon: 0.03												

FIG. 8: Pair-wise comparison matrix to estimate relative fire intensity for each facility

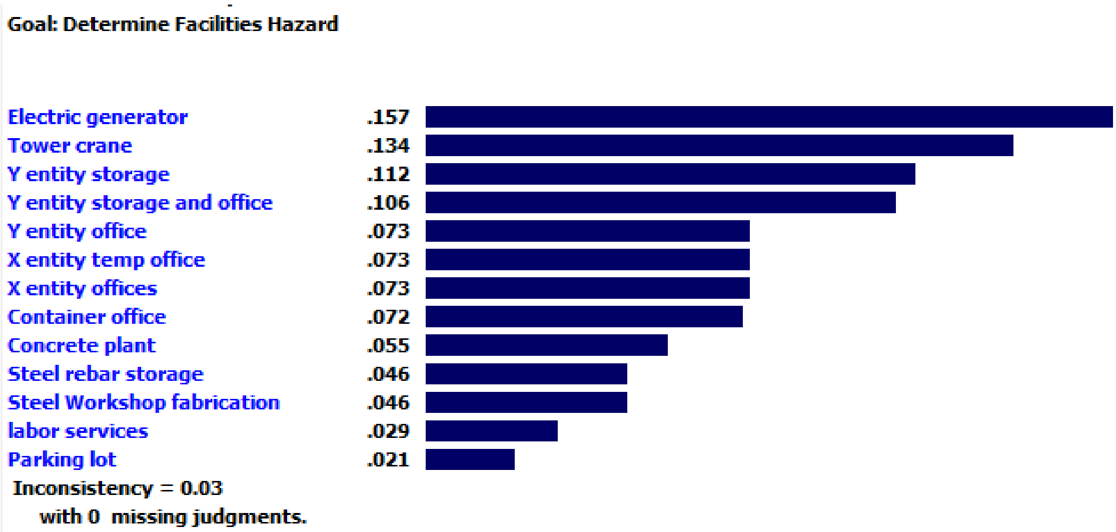

FIG. 9: Relative priorities of facilities according to main goal (estimating fire hazard intensity for each facility)

The values in the last column in TABLE 6 present the diagonal values in the hazard interaction matrix. The remaining values in the matrix that display the impact of each hazard source on each target within the construction site are determined by utilizing equation (1), which depends on the hazard intensity at the object itself (diagonal values in the matrix), the distances among the objects, and the hazard attenuation value as shown in TABLE 4. Also, due to the reasons of simplicity explained above, the hazard interaction matrix that was created will represent the conditional vulnerability of the potential targets too. The potential risk (r_{ij}) can thereafter be estimated by determining the mathematical product between the hazard and vulnerability matrices, as shown in TABLE 5. Once the risk interaction matrix is created, the next step is to perform matrix algebra in order to identify the relative global potential risk of each facility (ψ_i), which is later imported to GIS in order to visualize the variety of risk within the construction site and to identify the most at risk position inside it. This then requires more attention during the construction process. All of the matrix algebra calculations are shown in TABLE 5.

TABLE 4: Hazard interaction matrix

Facility No.	Facilities	F_1	F_2	F_3	F_4	F_5	F_6	F_7	F_8	F_9	F_{10}	F_{11}	F_{12}	F_{13}	F_{14}	F_{15}	F_{16}	F_{17}
F_1	Electric generator	4.00	3.95	3.61	3.60	3.50	3.47	3.53	3.50	3.52	3.23	3.80	3.82	3.54	3.58	3.62	3.62	3.73
F_2	Tower crane	3.36	3.41	2.98	2.97	2.87	2.84	2.90	2.88	2.93	2.59	3.23	3.18	2.90	2.96	2.88	3.07	3.09
F_3	Y storage	2.46	2.42	2.85	2.79	2.72	2.71	2.76	2.75	2.56	2.24	2.44	2.63	2.64	2.23	2.37	2.08	2.46
F_4	Y storage and office	2.30	2.26	2.64	2.70	2.60	2.56	2.57	2.58	2.35	2.15	2.26	2.48	2.54	2.12	2.17	1.92	2.35
F_5	Y office1	1.36	1.32	1.73	1.76	1.86	1.80	1.74	1.77	1.47	1.34	1.32	1.54	1.71	1.21	1.47	0.98	1.43
F_6	Y office 2	1.33	1.29	1.72	1.72	1.80	1.86	1.76	1.80	1.50	1.29	1.31	1.51	1.65	1.16	1.26	0.95	1.38
F_7	X temporary office 1	1.39	1.35	1.77	1.73	1.74	1.76	1.86	1.82	1.59	1.21	1.40	1.56	1.60	1.16	1.35	1.02	1.39
F_8	X temporary office 2	1.36	1.33	1.76	1.74	1.77	1.80	1.82	1.86	1.55	1.25	1.36	1.54	1.63	1.16	1.31	0.99	1.39
F_9	X offices	1.38	1.38	1.57	1.51	1.47	1.50	1.59	1.55	1.86	1.36	1.51	1.48	1.36	1.03	1.56	1.10	1.25
F_{10}	Container office	1.06	1.01	1.22	1.28	1.31	1.26	1.18	1.22	1.33	1.83	0.91	1.37	1.43	1.25	0.78	0.72	1.31
F_{11}	Concrete plant	1.20	1.22	0.99	0.96	0.86	0.85	0.94	0.90	1.05	0.48	1.40	1.13	0.84	0.78	1.23	0.99	0.95
F_{12}	Steel rebar storage	0.99	0.94	0.95	0.95	0.85	0.82	0.87	0.85	0.79	0.71	0.90	1.17	0.88	0.72	0.76	0.60	0.94
F_{13}	Steel workshop fabrication	0.71	0.66	0.96	1.01	1.02	0.96	0.91	0.94	0.67	0.77	0.61	0.88	1.17	0.65	0.50	0.33	0.85
F_{14}	Labor services	0.32	0.29	0.12	0.16	0.09	0.04	0.04	0.04	0.00	0.16	0.12	0.29	0.22	0.74	0.00	0.13	0.51
F_{15}	Parking lot	0.16	0.01	0.06	0.01	0.15	0.00	0.03	0.00	0.24	0.00	0.37	0.13	0.00	0.00	0.54	0.02	0.00
F_{16}	Construction building 1	1.62	1.66	1.23	1.22	1.12	1.09	1.16	1.13	1.24	0.89	1.59	1.43	1.16	1.39	1.48	2.00	1.41
F_{17}	Construction building 2	1.73	1.68	1.61	1.65	1.57	1.52	1.53	1.53	1.39	1.48	1.55	1.77	1.68	1.77	1.38	1.41	2.00

TABLE 5: Risk interaction matrix, potential risk (r_{ij}), and the implementation of matrix algebra to estimate relative global potential risk (ψ_i)

Facility No.	F_1	F_2	F_3	F_4	F_5	F_6	F_7	F_8	F_9	F_{10}	F_{11}	F_{12}	F_{13}	F_{14}	F_{15}	F_{16}	F_{17}	$\varphi^*_{i,.}$	χ^*_i	$\boldsymbol{\Psi^*_i}$
F_1	16	15.57	13.01	12.97	12.25	12.03	12.43	12.28	12.42	10.44	14.41	14.57	12.51	12.84	13.12	13.08	13.95	223.89	281.59	0.153
F_2	11.26	11.63	8.87	8.81	8.22	8.05	8.41	8.27	8.56	6.69	10.44	10.12	8.39	8.75	8.29	9.44	9.57	153.77	210.29	0.114
F_3	6.04	5.85	8.12	7.79	7.40	7.33	7.62	7.55	6.57	5.00	5.97	6.94	6.94	4.98	5.62	4.34	6.06	110.11	170.16	0.093
F_4	5.30	5.10	6.97	7.29	6.75	6.57	6.63	6.66	5.54	4.60	5.11	6.17	6.47	4.48	4.73	3.69	5.50	97.57	157.53	0.086
F_5	1.85	1.73	2.99	3.09	3.46	3.25	3.01	3.15	2.17	1.78	1.76	2.38	2.91	1.46	2.17	0.96	2.04	40.17	97.79	0.053
F_6	1.77	1.66	2.95	2.97	3.25	3.46	3.11	3.26	2.25	1.66	1.72	2.28	2.72	1.33	1.58	0.90	1.90	38.76	95.47	0.052
F_7	1.92	1.82	3.14	3.01	3.01	3.11	3.46	3.30	2.54	1.47	1.95	2.42	2.56	1.33	1.83	1.04	1.92	39.83	97.87	0.053
F_8	1.86	1.76	3.09	3.03	3.15	3.26	3.30	3.46	2.41	1.56	1.86	2.38	2.65	1.34	1.72	0.98	1.92	39.73	97.60	0.053
F_9	1.92	1.89	2.47	2.29	2.17	2.25	2.54	2.41	3.46	1.85	2.28	2.19	1.85	1.06	2.42	1.20	1.57	35.82	89.20	0.049
F_{10}	1.13	1.01	1.48	1.63	1.70	1.59	1.40	1.49	1.76	3.35	0.83	1.87	2.05	1.57	0.61	0.52	1.71	25.70	68.449	0.037
F_{11}	1.43	1.49	0.99	0.92	0.75	0.73	0.88	0.81	1.10	0.23	1.96	1.27	0.71	0.61	1.50	0.97	0.90	17.26	71.80	0.039
F_{12}	0.97	0.89	0.91	0.91	0.73	0.67	0.75	0.73	0.63	0.50	0.80	1.37	0.77	0.52	0.57	0.37	0.89	12.97	72.99	0.040
F_{13}	0.50	0.43	0.91	1.03	1.03	0.92	0.83	0.88	0.45	0.59	0.38	0.77	1.37	0.42	0.25	0.11	0.73	11.61	67.74	0.037
F_{14}	0.10	0.08	0.01	0.02	0.01	0.00	0.00	0.00	0.00	0.03	0.01	0.08	0.05	0.55	0.00	0.02	0.26	1.24	47.56	0.026
F_{15}	0.03	0.00	0.00	0.00	0.02	0.00	0.00	0.00	0.06	0.00	0.13	0.02	0.00	0.00	0.29	0.00	0.00	0.55	49.39	0.027
F_{16}	2.61	2.76	1.52	1.49	1.25	1.19	1.34	1.28	1.53	0.80	2.52	2.06	1.34	1.94	2.20	4.00	2.00	31.84	75.45	0.041
F_{17}	3.01	2.84	2.60	2.71	2.46	2.30	2.33	2.33	1.94	2.19	2.40	3.14	2.83	3.13	1.92	2.00	4.00	44.11	87.73	0.048
$\varphi^*_{.,j}$	57.70	56.51	60.04	59.96	57.62	56.70	58.04	57.86	53.38	42.75	54.54	60.02	56.13	46.33	48.83	43.62	54.92		1838.58	1.00

TABLE 6:Facilities hazard intensity

Facility	Description	Relative priorities	Normalized priorities	Fire hazard intensity
F_1	Electric generator	0.157	1	4.00
F_2	Tower crane	0.134	0.85	3.41
F_3	Y entity storage	0.112	0.71	2.85
F_4	Y entity storage & office	0.106	0.68	2.70
F_5	Y entity office 1	0.073	0.46	1.86
F_6	Y entity office 2	0.073	0.46	1.86
F_7	X entity temp office 1	0.073	0.46	1.86
F_8	X entity temp office 2	0.073	0.46	1.86
F_9	X entity offices	0.073	0.46	1.86
F_{10}	Container office	0.072	0.46	1.83
F_{11}	Concrete plant	0.055	0.35	1.40
F_{12}	Steel rebar storage	0.046	0.29	1.17
F_{13}	Steel workshop fabrication	0.046	0.29	1.17
F_{14}	Labor services	0.029	0.18	0.74
F_{15}	Parking lot	0.021	0.13	0.54
F_{16}	Building 1	---	---	2^*
F_{17}	Building 2	---	---	2^*

* The hazard intensity value is assigned based on the managers' suggestion.

The summation of each row as shown in TABLE 5 represents the potential risk generated by each facility (i) at the whole site ($\phi^*_{i,-}$ column), whereas the summation of each column represents the potential sensitivity of each target to the total risk generated from sources ($\phi^*_{-,j}$ last row in the table). The ($\varkappa^*_i$) and (ψ_i) columns in the table represent the global potential risk and relative global potential risk of each source (i) on the whole site respectively. It is clear from TABLE 5 that facility (F_1) has the most influence on the system compared with other facilities, with a relative global potential risk equal to 15.3 % followed by facility (F_2) with a relative global potential risk equal to 11.4%. This indicates that the risk consequences from facility (F_1) are the highest, whereas those generated from the two facilities (F_{14}) and (F_{15}) are the lowest. Moreover, TABLE 5 shows that facility (F_1) has the greatest potential risk in the plant, with a value equal to 223.9, whereas facility (F_{15}) has the lowest potential risk at the site with a value equal to 0.55. TABLE 5 also indicates that the greatest influence on the whole plant arises from facility (F_1) with a total value equal to 281.6, while the least influence on the whole plant is caused by facility (F_{14}) with a total value equal to 47.6. Also, the most dominant facility on the site that has a highest difference between potential risk ($\phi^*_{i,-}$) and potential sensitivity ($\phi^*_{-,j}$) is facility (F_1) followed by facility (F_2) (i.e. $\phi^*_{i,-} - \phi^*_{-,j}$), whereas the least dominant facility that has the lowest difference between potential risk ($\phi^*_{i,-}$) and potential sensitivity ($\phi^*_{-,j}$) is facility (F_{15}).

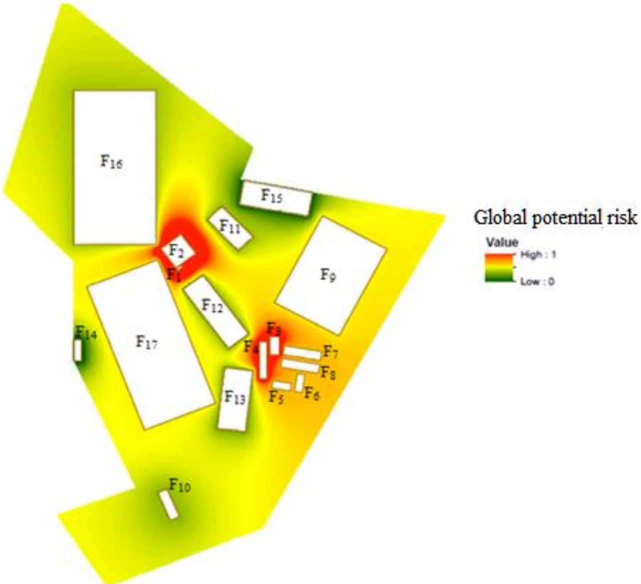

FIG. 10: Spatial variability of global potential risk within a site

FIG. 10 also displays the spatial variability of global potential risk within a construction site, the estimation of which is based on the global potential risk of facilities (ψ_i) and on an interpolation conducted utilizing IDW. It is obvious that the areas closer to the facilities with the highest global potential risk will have higher values of potential risk than those located far away. Hence, the most at risk position is located at approximately the middle of the site (around facilities F_1 and F_2) where these two facilities having the highest global potential risk. There is also another area around Y entity storages (F_3 and F_4) that has a high risk since these facilities have high relative global potential risk values compared to the remaining facilities (tagged in red color). Furthermore, it becomes obvious that the areas located near facilities (F_{14}) and (F_{15}) have the lowest risk (tagged in green). However, the remaining locations have approximately moderate risk, especially those that are very close to facilities with relatively moderate global potential risk values.

5. CONCLUSIONS

This paper presents a new methodology for visualizing construction site risk, generated by natural or technological hazard, based on developing hazard and vulnerability interaction matrices between potential sources and potential surrounding targets. The spatial variability of construction site risk is visualized by estimating the global potential risk of facilities obtained from the risk interaction matrix, which is in turn imported to a geographic information system (GIS) in order to generate the risk map for the whole construction site. The framework is implemented in a real case study for illustrative purposes. It consists in several facilities acting as hazardous source objects that are able also to become potential target objects in a 2D layout. The results indicated that the proposed framework is powerful and efficient due to its ability to visualize construction site risks due to hazard, and also to identify the positions most at risk within a construction site. The methodology then appears helpful in determining the best routes for evacuation in case of emergency and in assisting construction managers during the construction process, enabling them to avoid or at least minimize the consequences of risk's domino effects.

Currently, the proposed framework can be used in a same manner to visualize risks of other similar natural hazards (not only fire) within a construction site. It can then be expanded by finding worthy and significant criteria to evaluate vulnerability for each object within a construction site instead of utilizing assumption conditional vulnerability, which will enhance the precision of the risk visualization. Furthermore, identifying the best evacuation routes and emergency exits considering both risk and total evacuation time within a site can be further future endeavours. Moreover, integrating the risk generated by workers with the risk of natural hazards can also be another further future endeavor. The proposed framework is highly efficient in identifying the areas most at risk within a construction site, which will assist construction managers and planners to determine the best routes (with minimum risk) to follow in order to facilitate evacuation in cases of emergency.

ACKNOWLEDGEMENTS

The researchers acknowledge the École Spéciale des Travaux Publics (ESTP Paris) in France and An-Najah National University in Palestine for providing assistance, financial support and other requirements to complete this research. The theoretical developments also benefited from the Chinese-French program PHC-CaiYuanpei ("Havu-Risk: Chemical industrial plants & domino effect: hazards, vulnerability, risks & sustainability" 32114TE, 2014-2016).

REFERENCES

Ahmed, M., Jerez, S., Matasic, I., Prodhomme, G., Reimeringer, M., 2012. Explosions and Structural Fragments as Industrial Hazard: Domino Effect and Risks. Procedia Eng. 45, 159–166.

Akintoye, A.S., MacLeod, M.J., 1997. Risk analysis and management in construction. Int. J. Proj. Manag. 15, 31–38.

Banaitiene, N., Banaitis, A., n.d. Risk Management in Construction Projects.

Carr, V., Tah, J.H.., 2001. A fuzzy approach to construction project risk assessment and analysis: construction project risk management system. Adv. Eng. Softw. 32, 847–857.

Charriere, M.K.M., Bogaard, T.A., Mostert, E., 2012. Disaster Managers' Perception of Effective Visual Risk Communication for General Public.

Elbeltagi, E., Hegazy, T., 2003. Optimum layout planning for irregular construction sites. 5th CSCE Constr. Spec. ….

El-Rayes, K., Said, H., 2009. Global Optimization of Dynamic Site Layout Planning in Construction Projects. Constr. Res. Congr. 2009@.

Gao, M., Mo, J., He, G., 2007. A Simultaneous Route and Departure Time Choice Model for Evacuation Planning. Int. Conf.

Jannadi, O.A., Almishari, S., 2003. Risk Assessment in Construction. J. Constr. Eng. Manag. 129, 492–500.

Kang, L., Kim, S., Moon, H., Kim, H., 2013. Development of a 4D object-based system for visualizing the risk information of construction projects. Autom. Constr.

Kim, H., Lee, H., Park, M., Choi, B., 2013. Automated information retrieval for hazard identification in construction site. Proc. ASCE.

Mavroulidou, M., Hughes, S., Hellawell, E., 2004. A qualitative tool combining an interaction matrix and a GIS to map vulnerability to traffic induced air pollution. J. Environ.

Mebarki, a., Valencia, N., Salagnac, J.L., Barroca, B., 2012. Flood hazards and masonry constructions: a probabilistic framework for damage, risk and resilience at urban scale. Nat. Hazards Earth Syst. Sci. 12, 1799–1809.

Mebarki, A., Barroca, B., 2014. Resilience and vulnerability analysis for restoration after tsunamis and floods: the case of dwellings and industrial plants. Post-Tsunami Hazard Reconstr.

Mebarki, A., Jerez, S., Matasic, I., Prodhomme, G., 2014. Domino effects and industrial risks: integrated probabilistic framework–case of tsunamis effects. Tsunami Events and.

Mebarki, A., Valencia, N., 2012. Flood hazards and masonry constructions: a probabilistic framework for damage, risk and resilience at urban scale. Hazards Earth ….

Mitropoulos, P., Namboodiri, M., 2010. New method for measuring the safety risk of construction activities: Task demand assessment. J. Constr. Eng.

Raz, T., Michael, E., 2001. Use and benefits of tools for project risk management. Int. J. Proj. Manag.

Rozenfeld, O., Sacks, R., Rosenfeld, Y., Baum, H., 2010. Construction Job Safety Analysis. Saf. Sci. 48, 491–498.

Saaty, T., 2000. Fundamentals of decision making and priority theory with the analytic hierarchy process.

Sousa, V., Almeida, N.M., Dias, L.A., 2015. Risk-based management of occupational safety and health in the construction industry – Part 2: Quantitative model. Saf. Sci. 74, 184–194.

Zhang, L., Zhang, X., Ma, T., 2013. Management of Construction Schedules Based on Building Information Modeling Technology. Springer New York, pp. 81–88.

Zlatanova, S., Peters, R., Fendel, E.M., n.d. Proceedings of the 8 th International Conference on Geo-information for Disaster Management – Best Practices.

Zolfagharian, S., Irizarry, J., 2014. Current Trends in Construction Site Layout Planning. In: Construction Research Congress 2014. American Society of Civil Engineers, Reston, VA, pp. 1723–1732.